

Pneumatic Nozzle with Modified Internal Mixing Geometry

B. Schlinge^{*}, A. Mescher, P. Walzel

Laboratory of Mechanical Process Engineering, Technical University of Dortmund, Germany
britta.schlinge@bci.tu-dortmund.de, axel.mescher@bci.tu-dortmund.de and
peter.walzel@bci.tu-dortmund.de

Abstract

Twin-fluid atomizers with internal mixing operation require comparatively little energy and allow small drop sizes compared to the nozzle orifice diameters. For small drops a good mixing performance of the two phases inside the nozzle is necessary. Commercially available nozzle designs contain a bored mixing tube to disperse the gas into the continuous liquid phase. In contrast, a newly designed nozzle** is based on the distribution of the liquid into the gas flow by numerous capillaries. Liquid threads detach from the capillaries that are subsequently extended and attenuated by the coaxial gas stream. By that means a homogeneous gas/liquid flow is ensured leading to a spray without detectable pulsation within a wide range of operating parameters. Drop size distributions and pulsation frequencies of this nozzle design in comparison to a commercial nozzle are presented. Spray drying experiments were carried out with both atomizer geometries and the particle size distributions were compared.

Introduction

A large number of pneumatic nozzles mainly effervescent nozzles with different designs are known. Most commonly the pressurized air is dispersed into the continuous liquid phase in a mixing chamber consisting of a bored tube or a porous material. These nozzles show good spray performance for low air-to-liquid-ratios (ALR) [1, 2] compared to external mixing nozzles. However, for high ALR in the range of 1 to 10, the spray tends to pulsate [3, 4]. The reason for the undesirable spraying behavior may be an inhomogeneous gas/liquid flow in the mixing chamber. The flow regime inside the nozzle obviously becomes unstable, meaning a heterogeneous mixture of liquid and gas within the nozzle, finally leading to a pulsating spray [5]. Because of the temporary lower gas void fraction the amount of energy for fragmentation of drops at the orifice fluctuates. This leads to a broad drop size distribution. To avoid this problem, a new geometry of the mixing chamber is designed. Based on that concept the liquid is dispersed into the continuous gas phase by capillaries.

Experimental methods

In the present work, liquid is sprayed by compressed air with two different twin-fluid atomizers as shown in Figure 1 and Figure 2. The spray expands into ambience with $p = p_N$. For the commercial nozzle the gas enters through a side port. The liquid is fed from the top of the nozzle. The mixing chamber consists of a tube with a diameter of 2.6 mm for the liquid flow. The tube contains 12 bores, $d_{\text{hole}} = 1.5$ mm. Through these holes the gas is dispersed into the continuous liquid phase. This very simple and effective design was tested with orifice diameters of 1.0 and 1.5 mm.



Figure 1 commercial nozzle

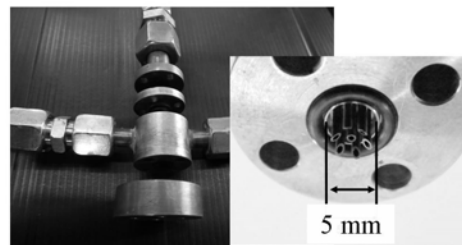


Figure 2 modified pneumatic nozzle, Multiple Capillary Nozzle (MCN)

The modified pneumatic nozzle, i.e. a multiple-capillary-nozzle (MCN), is shown in Figure 2. The gas enters through the two side ports into the mixing chamber. The liquid is introduced through multiple, in this case seven, capillaries with diameters of 0.5 mm, in contrary to [6] with only one capillary, surrounded by a coaxial gas-flow.

* Corresponding author: britta.schlinge@bci.tu-dortmund.de

** German patent application DE 102010 012 555.5-51

At the end of the capillaries jets are formed, which are attenuated and dispersed by the concurrent gas flow towards the main orifice, shown in Figure 3. Nozzle orifice diameters in the range of 1.0 to 2.0 mm were investigated with the somewhat more complicated MCN. Due to the design of the mixing chamber, the flow pattern, meaning the local liquid flow rate and gas content vs. time is almost constant over the cross-section. An unstable or pulsating spray is avoided over the whole range of operating parameters. The spray data are compared to those obtained with the commercial nozzle with equal orifice diameters and equal operation conditions.

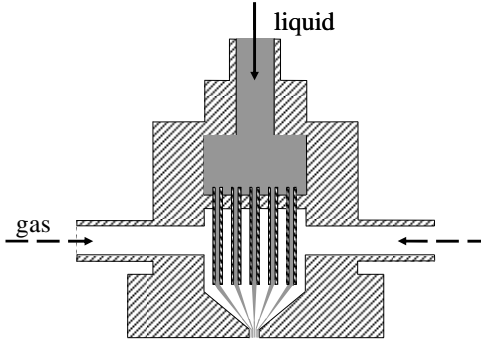


Figure 3 schematic flow pattern inside the MCN

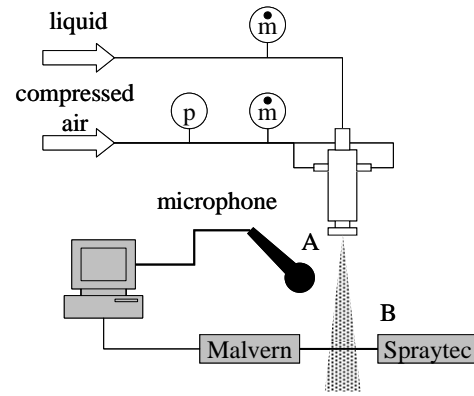


Figure 4 test rig, A: measurement for pulsation frequency, B: measurement for drop size distribution

The measurement program includes the drop size distribution and the pulsation frequencies observed at unstable process conditions. The experimental setup is presented in Figure 4. The sprayed liquids, water or mixtures of water and glucose covering the viscosity range of 1 to 100 mPas, are filled into a storage tank. The liquid holdup is gas-pressurized, in order to feed the liquid constantly to the nozzle. The gas (air) supply comes from the compressed air network of the lab. In both lines measurement devices for pressure and mass flow rate are installed. The investigated operating parameters cover differential pressures of up to 0.5 MPa and liquid mass flow rates of up to 40 kg/h. The gas flow rate was varied in the range of 0.5 to 15 kg/h. The resulting ALR is between 0.1 and 10.

Measurement of the spray pulsation frequency

For measurement of the pulsation frequency an acoustic measurement technique is designed. A pulsating nozzle generates noise [3, 7] that can be detected. The probable reason for acoustic emissions at the nozzle is periodic expansions of large gas bubbles. The recorded signal is analyzed regarding the characteristic frequency. A comparable measurement technique is used by thermal spraying for process control [8].

The signal is recorded by a microphone as shown in Figure 4 A. A capacitor microphone with cardioid characteristic is applied, in order to avoid recording of background noise. The signal is processed and analyzed by a Mathworks MATLABTM routine. Therefore the signal is compressed from 44 kHz to 6 kHz and imported to MATLAB. For analyzing the signal is converted to absolute values. For smoothing a finite impulse response filter is used, see Figure 5. This allows for a high approximation to the original signal, while an automatic analysis is enabled.

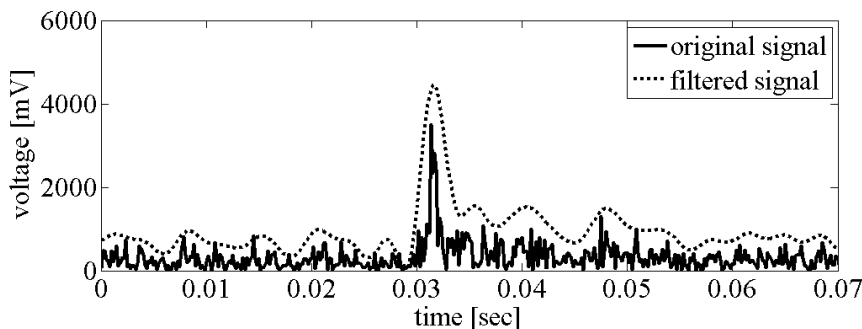


Figure 5 finite impulse response filter for commercial nozzle with $D = 1.5$ mm and the measurement point 0.5 MPa and $ALR = 5$

The filtered signal is processed by Fourier analysis. This operation transforms the filtered signal, which describes a function of continuous real arguments, to a continuous function of frequency. By that means the frequency distribution of the signal is calculated as shown in Figure 6. The prevalent frequency, i.e. the one with the highest amplitude, describes the frequency of the spray pulsation.

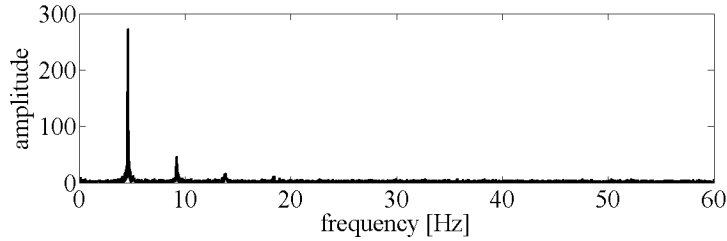


Figure 6 Fourier plot of the filtered signal for commercial nozzle with $D = 1.5$ mm and the measurement point 0.5 MPa and ALR = 5

In order to check mass flow fluctuations, the spray density vs. time was recorded by optical means. Pictures of the spray within a distance of 40 mm were taken with a rate of 240 pictures per second. The image interpretation is performed by a Mathworks MATLABTM routine. A threshold of the grey level within the pixels of the pictures are set to white, while the background is set to black. The white pixels of the spray are counted. In case of non-fluctuating sprays the quantity of white pixel is constant as all pixels within the given distance (total number $N_{tot} = 146,744$) to the nozzle are allocated as “white”. The pulsing of the spray leads to fluctuation of the white pixel number. The sum of white pixels at any instant is linked to the liquid holdup in the spray.

Measurement of the drop size distribution

For measurement of the drop size distribution the laser diffraction technique is used (Malvern 2000). As shown in Figure 4 B the Malvern 2000 is installed below the spray. The used lenses (focal length: 100 mm or 300 mm) allows the measurements of drop sizes between 1.9 to 530 μm . The distance between nozzle orifice and laser is constantly adjusted to 200 mm for all nozzle setups. The measurements were carried out continuously over 30 sec and threefold.

$$span = \frac{d_{90,3} - d_{10,3}}{d_{50,3}} \quad (1)$$

Narrow drop size distributions, i.e. small *span* (1) values are usually desired. In equation 1, $d_{50,3}$ describes the volumetric mean drop size. The values $d_{10,3}$ and $d_{90,3}$ represent the 10 %-percentile, the 90 %-percentile respectively, of the volumetric drop size distribution.

The drop size distribution obtained with two test liquids is measured. Water and aqueous solutions of glucose with water are used on one hand. The controlled gas front pressure is varied in the range of 0.2 to 0.5 MPa. The self-adjusting mass flow rate of the gas is measured. The liquid flow rate is adapted to the gas mass flow rate in order to obtain ALR ranges within 0.1 to 10.

On the other hand aqueous solutions of poly-vinyl-pyrrolidone (PVP) are sprayed. The PVP solutions allow for a considerable change of the mass content of solute. These solutions are therefore suitable feeds for the additional spray drying experiments. The atomization parameters are pressure, ALR and viscosity of the liquid. Viscosities of the liquid are changed by varying the PVP fraction within the aqueous solutions. The mass flow rate of the gas is varied by adjusting the front pressure and subsequently measured, while a constant liquid flow rate of 12 l/h is applied as the spray drying conditions can only be handled at limited solvent (water) mass flow. So the drop sizes are known in advance of the drying experiments.

Spray drying experiments and particle size distribution

For drying experiments aqueous solutions of poly-vinyl-pyrrolidone (PVP) are sprayed. Solutions of PVP Luvitec K30 (BASF SE) in the concentration range of 15 to 30 w/w-% are used. This leads to a viscosity range of 10 to 100 mPas. The experimental setup is shown in Figure 7. The atomizer is fed with a liquid flow rate of 12 l/h. The atomization gas is pressure controlled.

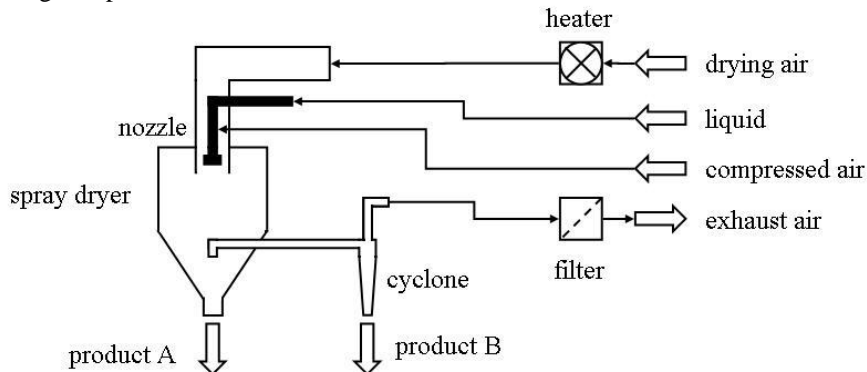


Figure 7 Spray drying system

The drying air has a flow rate of about 0.41 m³/s and a temperature of 170 °C / 110 °C at the dryer inlet / outlet. The coarse dry product is collected at the bottom of the drying chamber (A), while fine particles are separated from the gas via cyclone (B). At both collection points the mass of the product as well as the particle size distribution is measured. For the offline particle size measurement the laser diffraction technique is used. The particles are dispersed in silicon oil and are measured in a wet cell equipment and a Malvern Spraytec System.

Results and discussion

The measurements of the pulsation frequencies and the drop size distributions are done with two pneumatic nozzles with different mixing geometries. The data were obtained for given overhead gas pressures and for liquids with different viscosities. However, the results shown in this paper are exclusively based on the spraying experiments with water. The experiments revealed that the modified geometry of the MCN leads to a decreased pulsation tendency, especially at high ALR. Narrow drop size distributions could therefore be achieved. Regarding the mean drop size the MCN has only a moderate advantage compared to typical commercial nozzles.

Measurement of the pulsation frequency

The frequency measurements are carried out for each operation point. The presented results were gained for front pressures in the range of 0.2 to 0.5 MPa and for ALR varied from 0.1 to 10. The measured frequencies are shown for the commercial nozzle with D = 1.5 mm in Figure 8 and for the MCN with equal orifice diameter in Figure 9. For the commercial nozzle a pulsation tendency could be observed over a broad ALR-range. The frequency of pulsation decreases with increasing ALR at ALR > 1. At ALR = 0.5 the highest pulsation frequency for different gas-pressures was observed. By further decreasing the ALR the spray characteristic becomes stable. In contrast for the MCN no pulsations could be detected within the whole range examined. The spray is formed uniformly for the investigated range of ALR and gas-pressures.

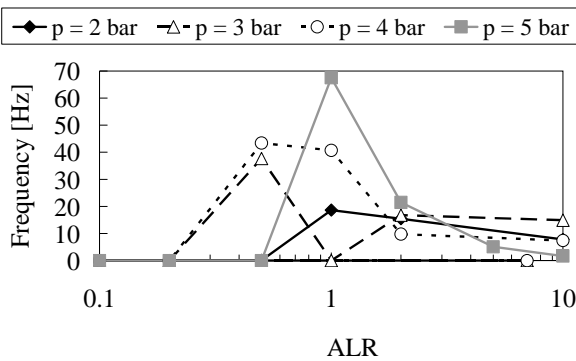


Figure 8 measurement results for pulsation frequency for commercial nozzle with D = 1.5 mm

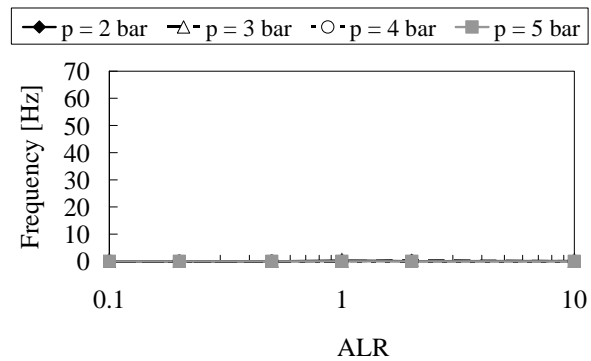


Figure 9 measurement results for pulsation frequency for the MCN D = 1.5 mm

In Figure 10 and Figure 11 the results are shown for the lower orifice diameter of 1.0 mm. The commercial nozzle showed a tendency to flow pulsations in the ALR range between 0.2 and 10 for all gas-pressure conditions. It can therefore be stated that lower nozzle diameters lead to flow pulsations at even lower ALR conditions. The MCN shows again no detectable pulsation.

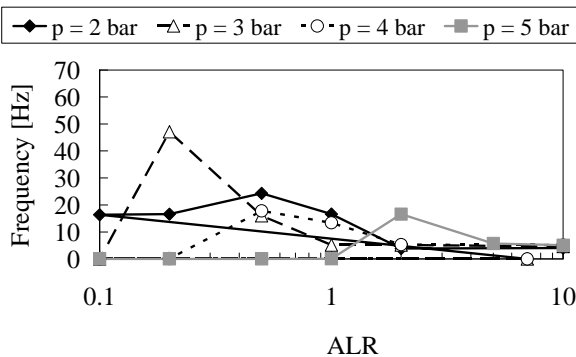


Figure 10 measurement results for pulsation frequency for commercial nozzle with D = 1.0 mm

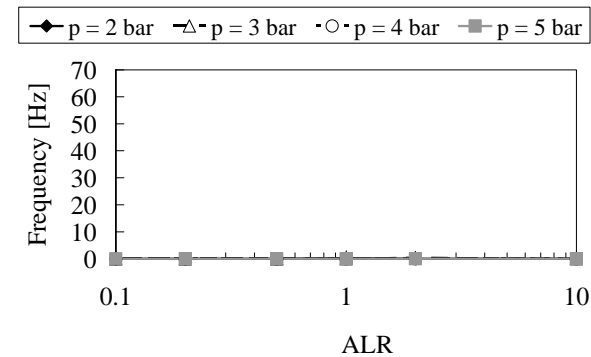


Figure 11 measurement results for pulsation frequency for the MCN D = 1.0 mm

As an example, for the commercial nozzle with D = 1.5 mm and Δp = 0.5 MPa as well as ALR = 5, the fluctuation of the white pixel number is shown in Figure 12. The results show a high variation of the liquid flow rate. In case of operating the MCN at same conditions, no fluctuations within the spray were visible.

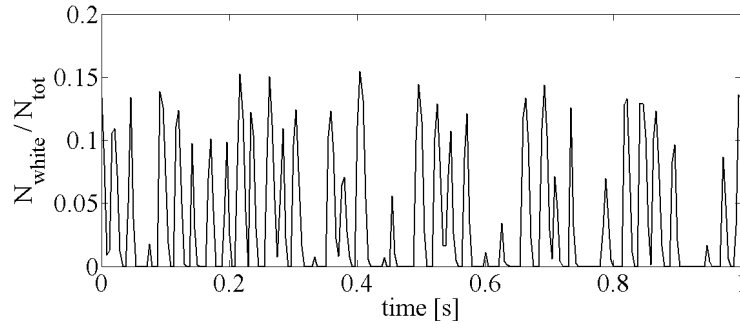


Figure 12 Number of white pixels within the spray up to a distance of 40 mm vs time for the commercial nozzle with $D = 1.5$ mm, $\Delta p = 0.5$ MPa and ALR = 5

Measurement of the drop size distribution

The drop size and *span* data were exclusively measured for water and in a gas-pressure range from 0.2 to 0.5 MPa. The ALR-range again resulted in 0.1 to 10. The results for both pneumatic nozzles with orifice diameters of 1.5 mm are given in Figure 13 and Figure 14. With increasing gas-pressure and ALR the mean drop size increases as expected for both designs. The mean drop size is comparable for both nozzles.

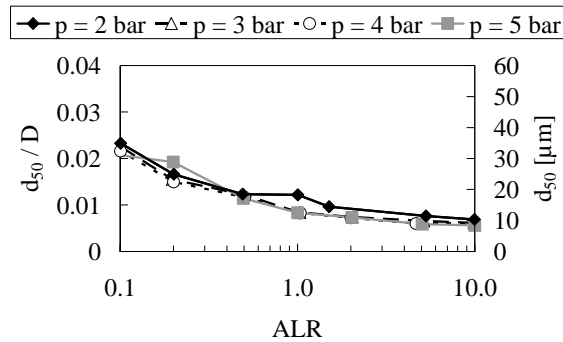


Figure 13 mean drop size of the commercial nozzle $D = 1.5$ mm

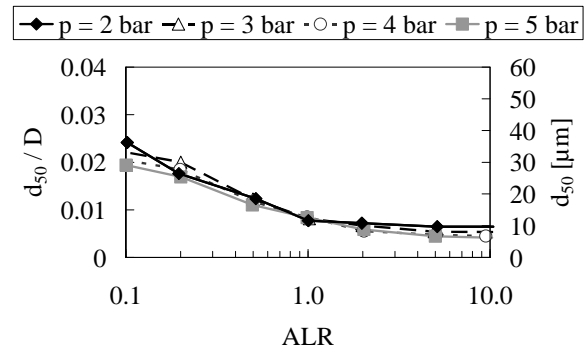


Figure 14 mean drop size of the MCN $D = 1.5$ mm

In Figure 15 and Figure 16 the *span* values are shown for both nozzles. The MCN shows constant span values of about 2 for all investigated ALR and gas-pressure conditions. For the commercial nozzle the *span* distinctly increases to a level of up to 9 at high ALR.

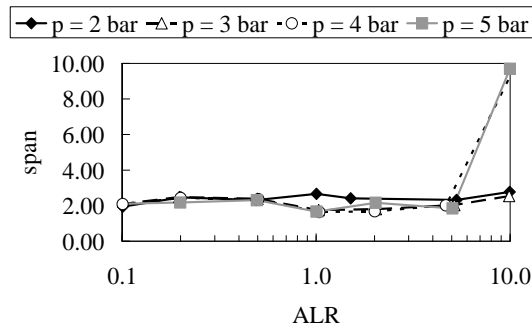


Figure 15 measured *span* of the commercial nozzle $D = 1.5$ mm

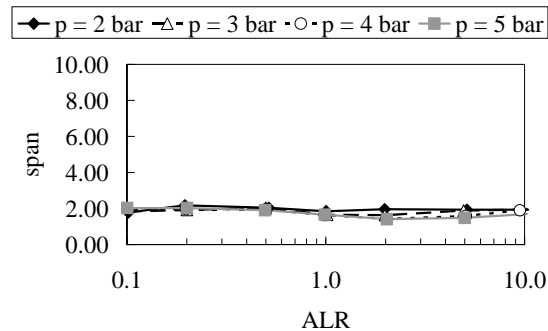


Figure 16 measured *span* of the MCN $D = 1.5$ mm

For nozzle orifice diameters of 1.0 mm a similar behavior was observed, as the mean drop size increases for the commercial nozzle while also an increasing drop size is detected for the MCN, see Figure 17 and Figure 18. Even though the MCN shows best performance at low ALR it must be stated, that the modified nozzle geometry shows no significant advantage regarding the drop size over the full ALR range.

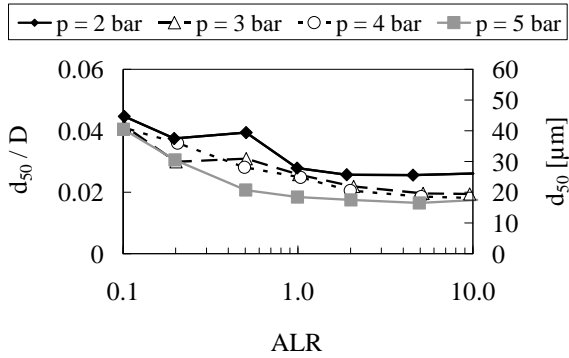


Figure 17 measured mean drop size of the commercial nozzle $D = 1.0$ mm

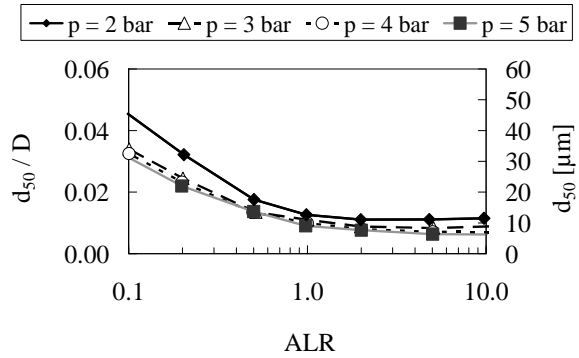


Figure 18 measured mean drop size of the MCN $D = 1.0$ mm

The width of the drop size distribution is shown for both pneumatic nozzles in terms of the *span*, see Figure 19 and Figure 20. For the commercial nozzle the *span* increases at higher ALR. For ALR-values below 1, the *span* reaches a constant value of 2. In contrast to the MCN with an orifice diameter of 1.5 mm, the smaller orifice diameter leads to slightly increased *span*-values. A trimodal drop size distribution was observed for higher ALR. In the next step of our work the change of drop size distribution as a function of the orifice diameters shall be explained by investigating the flow regimes inside the MCN. A nozzle with a transparent mixing chamber will be used for the characterization of thread disintegration.

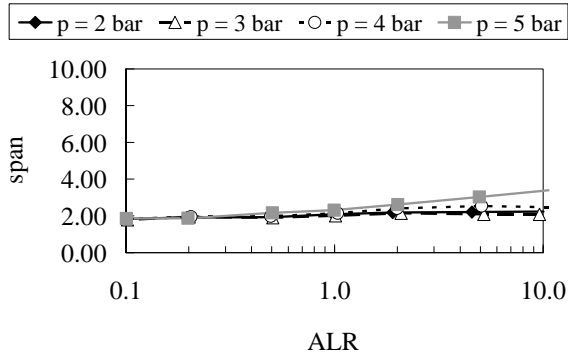


Figure 19 measured *span* of the commercial nozzle $D = 1.0$ mm

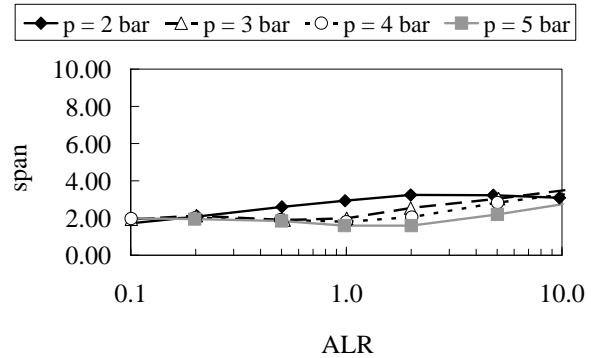


Figure 20 measured *span* of the MCN $D = 1.0$ mm

For spray drying experiments PVP K30 is used. The spray drying experiments are carried out with the commercial nozzle and the MCN with orifice diameter of 1.5 mm. So the drop size distributions and the *span* are measured with PVP K30 for the operation parameter inside the spray dryer. The results for the mean drop size are shown for the commercial nozzle in Figure 21 and for the MCN in Figure 22 and for the *span* in Figure 23 and Figure 24. The mean drop sizes and the *span* are in the same range for both nozzles designs. By increasing the viscosity of the liquid the *span* increases for both nozzles designs.

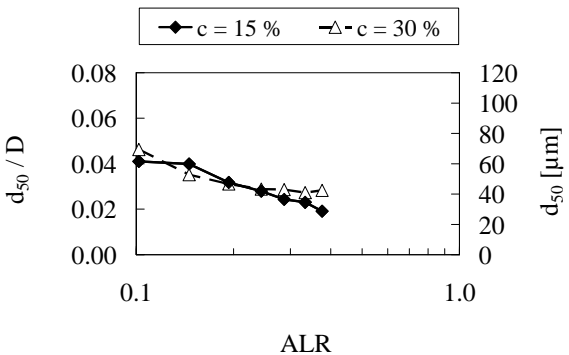


Figure 21 measured mean drop size with PVP K30 of the commercial nozzle $D = 1.5$ mm

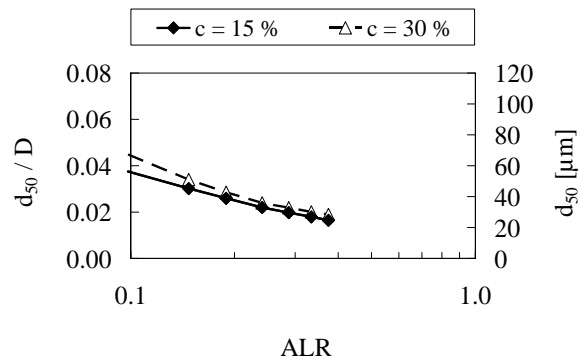


Figure 22 measured mean drop size with PVP K30 of the MCN $D = 1.5$ mm

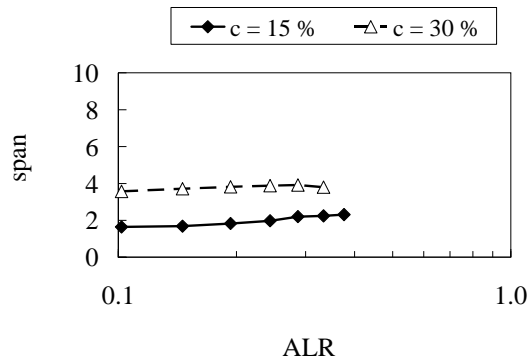


Figure 23 measured span of the commercial nozzle D = 1.5 mm

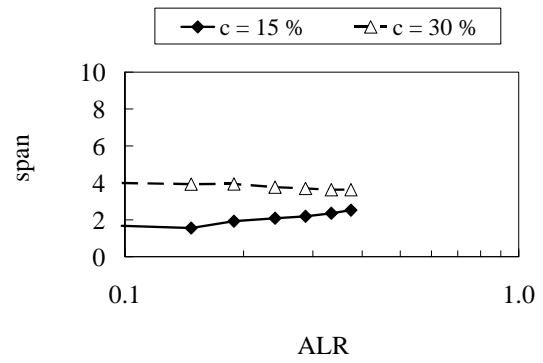


Figure 24 measured span of the MCN D = 1.5 mm

Spray drying experiments

In the spray drying experiments particles are collected at two points in the plant. The product of the spray dryer bottom shows a broader size distribution compared to the cyclone product, because of the classification of the particles in the cyclone. The yield of the spray drying process is comparatively high with 39 - 60 % for the commercial nozzle and 34 - 48 % for the MCN. Summarizing both pneumatic nozzles show a good performance in spray drying PVP solutions.

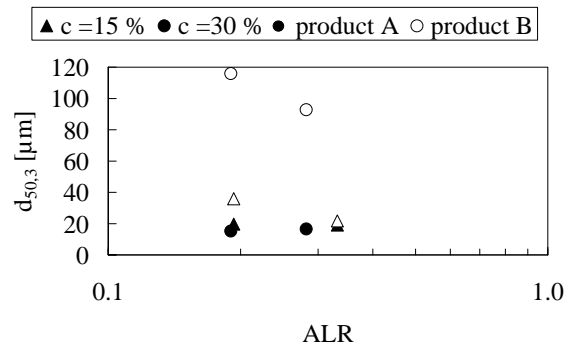


Figure 25 mean particle sizes for commercial nozzle D = 1.5 mm

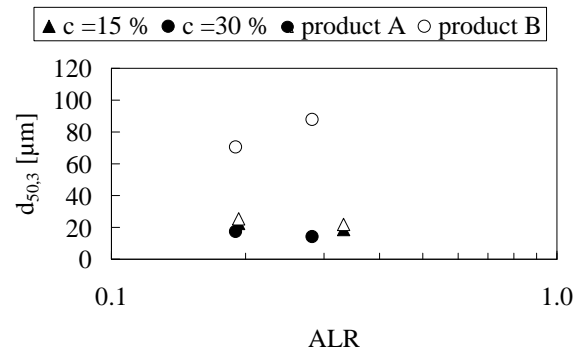


Figure 26 mean particle sizes for MCN D = 1.5 mm

The measured particle sizes, Figure 25 and Figure 26, show comparable results regarding the particle size distributions. This confirmed the results of the drop size measurements. Due to agglomeration the particles from the spray dryer are somewhat larger compared to the droplets. This could also be confirmed under the microscope by the morphology of the particles.

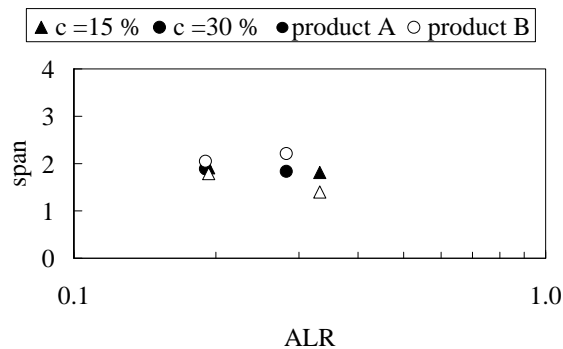


Figure 27 measured span of the commercial nozzle D = 1.5 mm

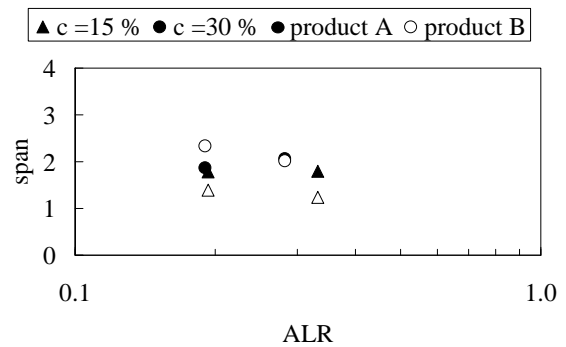


Figure 28 measured span of the MCN D = 1.5 mm

The measured span is shown for the particle size distribution of the spray drying with both pneumatic nozzles in Figure 27 and Figure 28. In determination of the mean particle size and the span the PSD the product A (tower) as well as B (cyclone) were considered. The width of the particles size distributions is in the same range as obtained from the drop size measurements. Both pneumatic nozzles show good spray drying performance in the considered interval of ALR.

Summary and Conclusions

The results of the drop size measurements for both pneumatic nozzles show comparable results for water. However, the width of the drop size distribution, namely the *span*, is somewhat lower when using the MCN with an orifice diameter of $D = 1.5$ mm and high ALR. The pulsation tendencies of the sprays instead, behave differently. No flow pulsations of the MCN-spray could be observed for an extended range of gas-pressures and ALR conditions. In contrast the commercial nozzle shows a strong tendency to flow pulsation, especially at higher ALR and at low orifice diameter. In spray drying both nozzles show a good spraying performance and the produced particle sizes were comparable.

Summarizing, it can be stated that for low ALR, especially below 1, the two pneumatic nozzles show comparable behavior regarding drop size and *span*. However, the MCN shows a significantly lower tendency to flow pulsations compared to the commercial nozzle. Therefore especially for the production of small particles by high ALR-conditions and low orifice diameters, the MCN may be advantageous compared to classical designs of twin-fluid-atomizers.

Acknowledgements

The authors want to thank the group KIT of Prof. Schuchmann for assistance in spray drying experience and BASF SE for providing Luvitec K30.

Nomenclature

ALR	air to liquid ratio [$\text{kg}_{\text{air}} / \text{kg}_{\text{liquid}}$]
c	concentration [w/w %]
D	diameter of the orifice of the nozzle [m]
$d_{50,3}$	volumetric averaged drop size [m]
$d_{90,3}$	drop size represent the 10 %-percentile of the volumetric drop size distribution [m]
$d_{10,3}$	drop size represent the 90 %-percentile of the volumetric drop size distribution [m]
d_{hole}	diameter of the bores inside the commercial nozzle [m]
N_{tot}	total number of pixels [-]
N_{white}	number of white pixels [-]
p	pressure [$\text{kg}\cdot\text{m}^{-1}\cdot\text{s}^{-2}$]
p_N	ambient pressure [$\text{kg}\cdot\text{m}^{-1}\cdot\text{s}^{-2}$]

References

- [1] Sutherland, J. J., Sojka, P. E., Plesniak, M. W., *International journal of multiphase flow*, 23 (5): 865–884, (1997)
- [2] Lörcher, M., Schmidt, F., Mewes, D., *Atomization and Sprays*, 15:145-168, (2005).
- [3] Luong, J. T. K., Sojka, P. E., *Atomization and Sprays*, 9 (1): 87-109, (1999).
- [4] J. Schröder, M. Schlender, P. E. Sojka, V. Gaukel, H. P. Schuchmann, *ILASS-Europe*, Brno, CZ, 2010.
- [5] J. Jedelsky, M. Jicha, *Atomization and Sprays*, 18 (1): 49-83, (2008).
- [6] S. Groom, *PhD Thesis*, TU Dortmund, 2006.
- [7] J. M. Chawla, *ICLASS*, (1985).
- [8] B. Wielage, C. Rupprecht, G. Paczkowski, *Mat.-wiss. U. Werkstofftech.*, 39 (1): 93-98, (2008).